UCLouvain

epl

LMECA2640: Mechanics of composite materials

Studying the effective properties of composite materials through several approaches

Work performed by:

Vansnick François (74871900)

Abstract

This report was prepared with the help of AI tools to improve the clarity and readability of the text for the reader. All content, analyses, and reflections presented here are original and reflect the product of my personal work, course notes or internet research. AI tools were used responsibly and solely to ensure the quality of the writing.

Introduction

Composite materials are increasingly used for their mechanical properties, which are better to ordinary materials because they combine the advantages of their different constituents. A composite is generally made of a matrix reinforced by inclusions such as fibers or particles. This composition leads to, for example, improved rigidity and mechanical strength. These materials are used in many applications, the most common are aerospace, automotive, and biomedical. Therefore, the study of their behavior is essential to develop and optimize their mechanical performance. To achieve this, this report is structured in three main parts. First, a mean-field homogenization approach, implemented using a code developed by myself, focusing on spherical inclusions in a matrix. Second, an analysis with Digimat-MF software to take into account ellipsoidal inclusions of different aspect ratios and orientations. And finally, a full-field homogenization study is carried out with Digimat-FE, applied to a periodic lattice structure.

The mechanical properties of a composite material strongly depend on the type of inclusions (shape, size, orientation) as well as the matrix and material properties. This sensitivity to the microstructural configuration makes the analytical or numerical study of the behavior of these materials essential. But they are even more so when the material itself is no longer solid and this brings us to the concept of lattice structures, where geometry plays a central role in the mechanical response. In some materials, the microstructure is combined with a periodic geometry such as a honeycomb structure and this leads to unique mechanical behaviors that are impossible to obtain with dense materials.

Most lattice structures are made using additive manufacturing, also known as 3D printing. However, there are several types and each has its own advantages and disadvantages. The principle is simple and relies on a layer-by-layer printing process that allows the creation of complex and hollow structures. A lattice is defined as a periodic structure composed of repeating cubic and spherical unit cells that form complex architectures from a beam framework. Depending on the material there are several manufacturing techniques:

- **Fused deposition modeling** or **Fused filament fabrication** (like home 3D printers) is a method that simply deposits a filament of molten material layer by layer. It's cheap and supports a large range of thermoplastic materials. However, its resolution is limited to the submillimeter scale that making it more suitable for large-scale lattice or rapid prototyping rather than high-precision applications.[1][2]
- Other processes more suited to metals and nylon are based on powder printing, such as **Selective laser sintering** or **Selective laser melting**. These techniques use a laser to melt and fuse powder particles at specific locations, resulting in good resolution and mechanical homogeneity but the problem is that they are very expensive. They are commonly used in sectors such as biomedical engineering (scaffolding) and motorsport (lightweight parts in Formula 1).[2]
- **Electron beam melting** (EBM) is a similar process to electron beam melting (SLM), the only

difference being that it uses an electron beam instead of a laser, and therefore must operate in a vacuum. While it offers even greater precision and lower residual stress, it is also more expensive and limited to conductive materials.[2]

- Resin-based photopolymerization techniques, such as **Stereolithography** (SLA) and especially **Digital light processing** (DLP), offer an excellent compromise between cost, precision, and material diversity. DLP uses a digital light projector to cure an entire layer of resin in one go, unlike SLA, which uses a single-spot UV laser. This allows for rapid production and excellent resolution (down to a few hundred microns or less). This method is widely considered the standard for manufacturing polymer network-based materials. Furthermore, minor layer-to-layer variations can be corrected by adjusting the beam diameter or exposure time.[3][4]

- Finally, **PolyJet printing** allows for the creation of multi-material networks by projecting tiny droplets of photopolymer resin that instantly harden under UV light. This technique makes it possible to create structures with spatially variable mechanical properties, such as different stiffness at each point of the material, and this is particularly useful in biomechanics for example.[3]

Polymer lattice structures are therefore primarily designed to reduce weight or optimize stiffness. However, there is an even higher class called lattice metamaterials, whose behavior is improved by modifying their internal geometry. Unlike traditional materials, their properties such as rigidity, Poisson's ratio and especially the propagation characteristics of sound and electromagnetic waves no longer depend on the composition, but also and mainly on the architecture of the cells of the material itself. A lattice metamaterial is therefore an adaptable periodic structure that allows for unique properties such as a negative Poisson's ratio (auxeticity), programmable stiffness and directional deformation.[6]

Thanks to their structure, metamaterials can, for example, control wave propagation, making them very effective in areas such as acoustics, vibration isolation, and electromagnetic shielding. For example, phononic and acoustic metamaterials can filter or block specific sound frequencies, which could help reduce noise in vehicle cabins, for example. While electromagnetic metamaterials, often inspired by similar reticular principles, can manipulate light and radio waves, allowing phenomena such as masking or negative refractive indices, which would allow flat eyeglass lenses that still focus light.[6][7]

Finally, based on the understanding of lattice metamaterials, this project aims to evaluate the influence of inclusion characteristics, in terms of volume fraction and shape, on the effective properties of composite materials using different modeling approaches. One of the main objectives is to determine the volume fraction of inclusions required to achieve a 60% stiffness improvement compared to the pure matrix, and to compare the results at analytical, semi-analytical and numerical scales, with an emphasis on the multi-scale potential of lattice composites.

Part 1: Mean field homogenization for a matrix reinforced with spherical stiffer inclusions

To model the material behavior with Mori-tanaka model, we must first obtain the basic mechanical properties of the material for the matrix and inclusions. For the inclusions, we will use glass as requested in the statement. For the matrix, we will choose the most commonly used polymer in Selective laser sintering, namely Nylon/PA 12. We obtain precise data via the Granta Edupack software, and we will be able to compare the results obtained via our code with those of Granta. Finally, We used the Mori-Tanaka model with closed-form expressions presented in Chapter 5 (pages 17–18), which relies on several important assumptions:

- The inclusions are spherical, rigid, isotropic, and distributed homogeneously in the matrix
- The matrix is also isotropic and linear elastic
- The deformation field is assumed to be uniform in the inclusions
- Interactions between inclusions are not explicitly considered, which limits the validity of the model to moderate volume fractions (generally less than 30%).

Material	Young's Modulus (GPa)	Poisson's Ratio	μ (GPa)	K (GPa)	Density (kg/m^3)
Nylon/PA12	1,215	0,414	0,4285	2,605	1010
Low E-Glass	70	0,215	28,75	40,85	2465

Table 1: Material properties

These values come from Granta Edupack but it is also possible to calculate them using the following formulas:

$$K = \frac{1}{3}\frac{E}{(1-2\nu)} \quad and \quad \mu = \frac{E}{2(1+\nu)}$$

The following graph shows the evolution of the normalized mechanical properties as a function of the inclusion rate. It compares the direct Mori-Tanaka model to an incremental version, which is more accurate at high inclusion rates. First, we notice an increase in Young's Modulus as expected since the rigidity of the glass is much higher than that of the polymer matrix. The direct Mori-Tanaka model is less efficient because it underestimates the value of the different coefficients. This is explained by the fact that the direct model assumes too ideal homogeneity, which limits its validity to low concentrations.

Since the Mori-Tanaka model is only valid for a number of inclusions less than or equal to 30%, we compared the results of the two models with the values found on the Granta-Edupack software. As can be seen in the table below 3, the incremental model is quite close to the real values with about 4% error, the direct model has about 6% error.

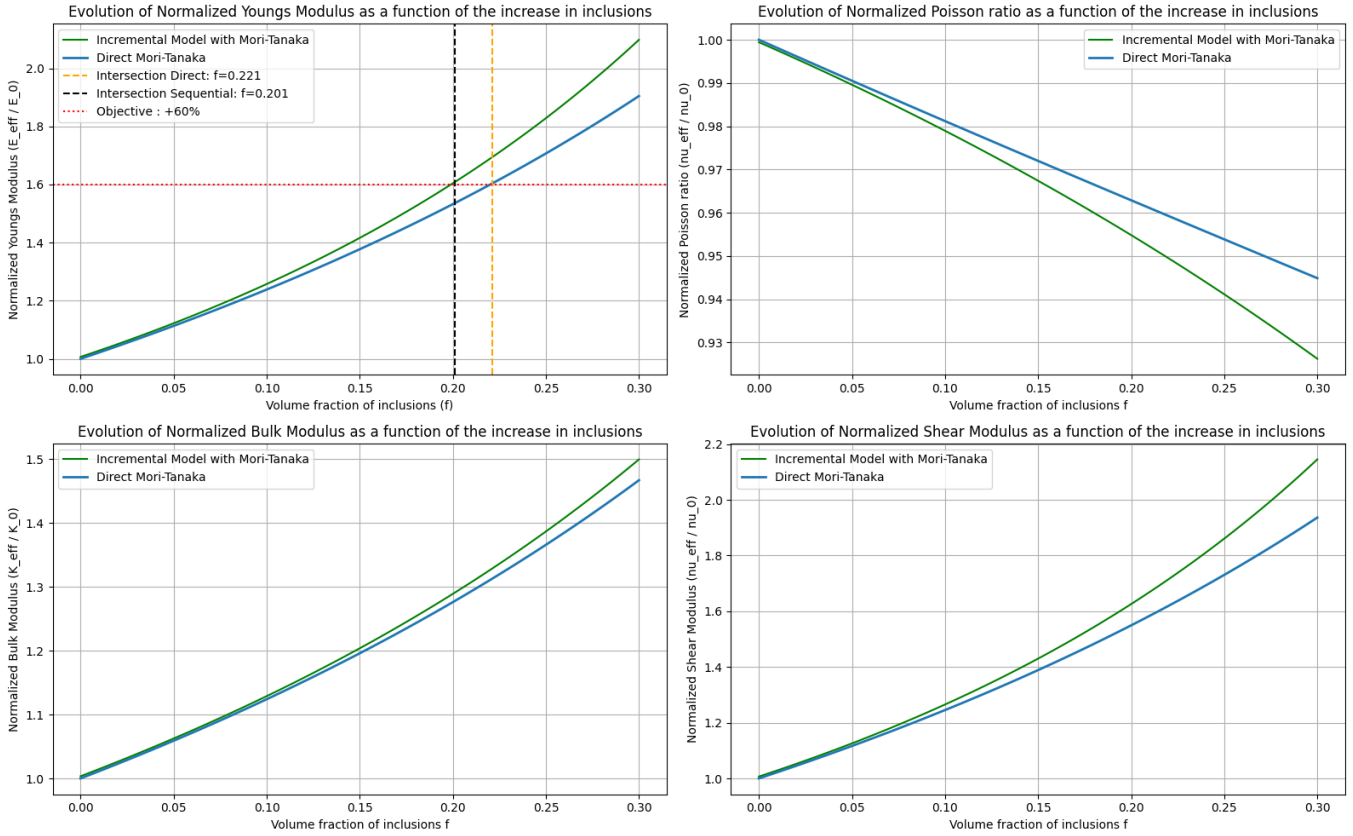

Figure 1: Graph of the evolution of mechanical properties as a function of the percentage of inclusions

A decrease in Poisson's ratio ν is also observed in both models, particularly in the incremental model. This is explained by the fact that inclusions are less compressible than the matrix, making the composite generally stiffer under volumetric deformation. The volumetric modulus of elasticity K increases with the inclusion ratio, but for this property, the results of the direct and incremental models are very similar, with a negligible difference over the entire range of volume fractions studied. This is explained by the fact that K is less sensitive to the effects of progressive interactions than the moduli E or μ.

Model	Young's Modulus (GPa)	Poisson's Ratio	μ (GPa)	K (GPa)
Direct M-T	2,321	0,399	0,830	3,822
Incremental M-T	2,557	0,391	0,919	3,907
Experimental value	2,46	0,414	0,922	4,765

Table 2: Material properties with different models at 30% of inclusions

Finally, the top left graph shows that the stiffness is improved by 60% compared to that of the matrix for an inclusion rate of 20.1% with the incremental method, and 22.1% with the direct Mori-Tanaka method. It can be seen that at this inclusion level, the values obtained by the two methods are relatively close. Moreover, the increase in stiffness (+60%) is significantly greater than the decrease in Poisson's ratio (-4%), highlighting the effectiveness of the reinforcement.

Part 2: Mean field homogenization for a matrix reinforced with spheroids inclusions for different orientations

In this second part of the study we modeled spheroidal inclusions which introduces geometric anisotropy, unlike the spheres used in the first part. Two distinct cases of orientation were studied, inclusions oriented unidirectionally (UD), i.e. aligned in our case along direction 11 and inclusions oriented randomly in space .

For the simulations, we used the Digimat-MF software. In the unidirectional case, the inclusions were oriented along axis 11 and a mechanical stress was applied in the same direction in order to extract the effective properties of the material. Since for this study, we assume that we are in the linear elastic case, the value of the imposed strain has no influence on the results. This therefore makes it possible to work indifferently with stresses or imposed strains, without altering the final mechanical constants. The obtained apparent Young's modulus were then normalized with the Young's modulus of the matrix to facilitate comparison between the different configurations. However, Digimat does not allow automatic calculation of multiple stiffness values for different aspect ratios or inclusion percentages in the same study. It was therefore necessary to run the calculations one by one for each value and then manually copy the results into an Excel file, which allowed the graphs to be generated directly. It is also important to note that Digimat encountered crashes for an aspect ratio of 0.001, which is why the analysis starts here from 0.01.

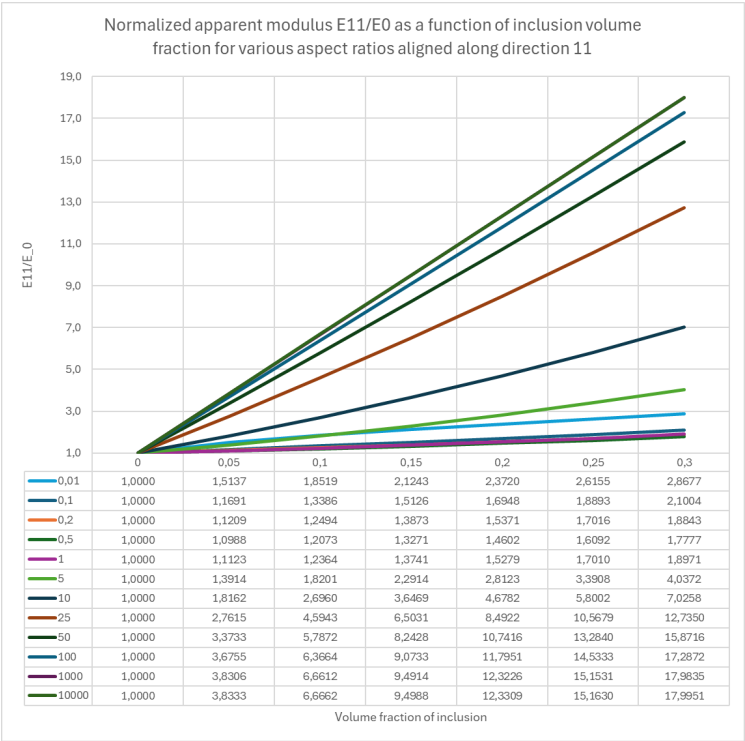

(a) Normalize apparent modulus E11, with UD inclusions

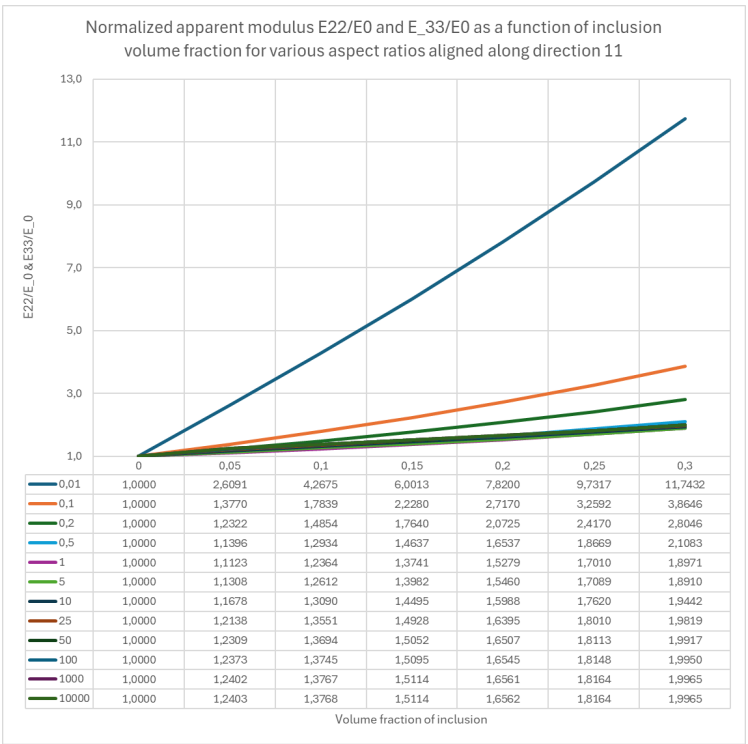

(b) Normalize apparent modulus E22 & E33, with UD inclusions

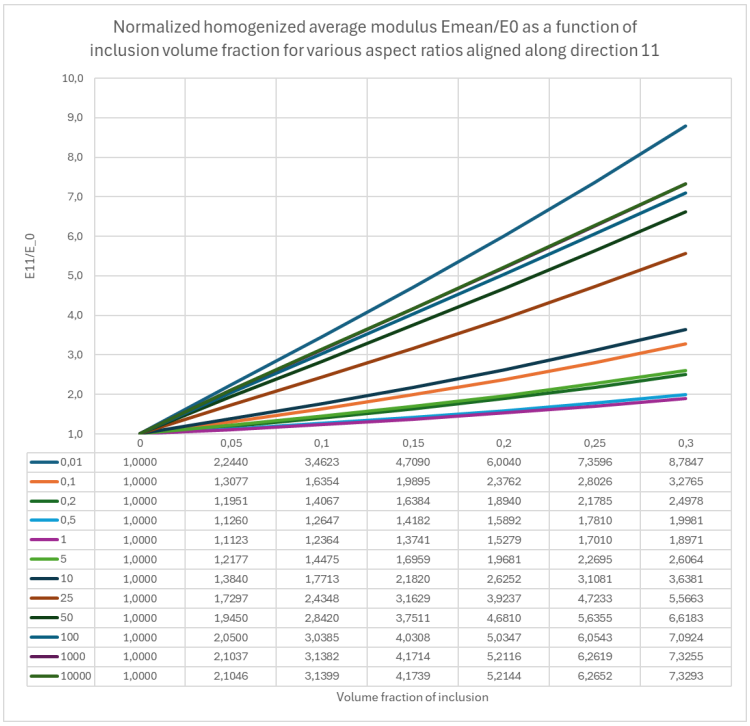

	0	0,05	0,1	0,15	0,2	0,25	0,3
0,01	1,0000	2,2440	3,4623	4,7090	6,0040	7,3596	8,7847
0,1	1,0000	1,3077	1,6354	1,9895	2,3762	2,8026	3,2765
0,2	1,0000	1,1951	1,4067	1,6384	1,8940	2,1785	2,4978
0,5	1,0000	1,1260	1,2647	1,4182	1,5892	1,7810	1,9981
1	1,0000	1,1123	1,2364	1,3741	1,5279	1,7010	1,8971
5	1,0000	1,2177	1,4475	1,6959	1,9681	2,2695	2,6064
10	1,0000	1,3840	1,7713	2,1820	2,6252	3,1081	3,6381
25	1,0000	1,7297	2,4348	3,1629	3,9237	4,7233	5,5663
50	1,0000	1,9450	2,8420	3,7511	4,6810	5,6355	6,6183
100	1,0000	2,0500	3,0385	4,0308	5,0347	6,0543	7,0924
1000	1,0000	2,1037	3,1382	4,1714	5,2116	6,2619	7,3255
10000	1,0000	2,1046	3,1399	4,1739	5,2144	6,2652	7,3293

(a) Normalize apparent average modulus E_mean, with UD inclusions

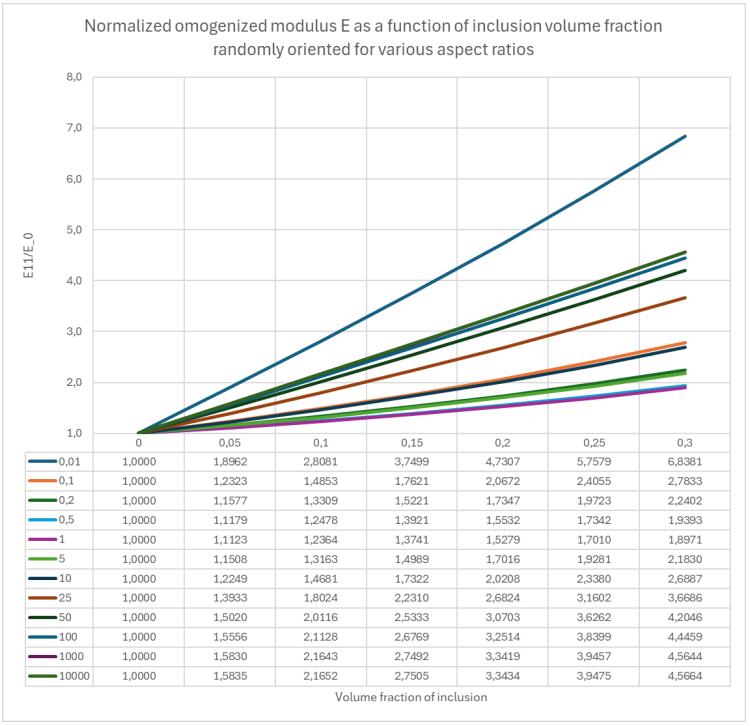

	0	0,05	0,1	0,15	0,2	0,25	0,3
0,01	1,0000	1,8962	2,8081	3,7499	4,7307	5,7579	6,8381
0,1	1,0000	1,2323	1,4853	1,7621	2,0672	2,4055	2,7833
0,2	1,0000	1,1577	1,3309	1,5221	1,7347	1,9723	2,2402
0,5	1,0000	1,1179	1,2478	1,3921	1,5532	1,7342	1,9393
1	1,0000	1,1123	1,2364	1,3741	1,5279	1,7010	1,8971
5	1,0000	1,1508	1,3163	1,4989	1,7016	1,9281	2,1830
10	1,0000	1,2249	1,4681	1,7322	2,0208	2,3380	2,6887
25	1,0000	1,3933	1,8024	2,2310	2,6824	3,1602	3,6686
50	1,0000	1,5020	2,0116	2,5333	3,0703	3,6262	4,2046
100	1,0000	1,5556	2,1128	2,6769	3,2514	3,8399	4,4459
1000	1,0000	1,5830	2,1643	2,7492	3,3419	3,9457	4,5644
10000	1,0000	1,5835	2,1652	2,7505	3,3434	3,9475	4,5664

(b) Normalize apparent modulus E11, randomly oriented inclusions

In the UD case, the material behavior becomes clearly anisotropic. A marked difference is observed between the Young's modulus in the 11 direction (E11), aligned with the inclusions, and those in the transverse directions (E22 and E33). This difference is even more pronounced when the aspect ratio moves away from unity (i.e. 0.01 or 10000). This difference is logical, because oriented inclusions induce preferential reinforcement in the direction of their alignment. More precisely, E11 is maximized for very high aspect ratios, with a maximum value reached around $AR = 10,000$. Conversely, the transverse modulus E22 and E33 are maximized for very low aspect ratios, typically around $AR = 0.01$. This shows that very flattened inclusions can effectively reinforce the directions perpendicular to the alignment axis.

Another interesting point is that the results for $AR = 100, 1000$ and 10,000 are relatively close with respect to E11, which indicates that the strengthening effect in the principal direction reaches a kind of saturation from a certain slenderness threshold. Finally, if we consider a more global approach, for example by observing the average of the Young's moduli in the three principal directions, we notice that the aspect ratio which gives the highest apparent modulus is $AR = 0.01$. This means that, in the studied configuration, very flattened inclusions offer better overall stiffness than very elongated inclusions in a single direction. In summary, the results show that inclusions with an extreme aspect ratio, either very large or very small, allow to optimize the mechanical properties of the material. Highly elongated inclusions effectively reinforce the direction of their alignment, while very flattened inclusions are more effective in reinforcing the transverse directions and improving the overall behavior of the composite. Intermediate-shaped inclusions, on the other hand, turn out to be less effective overall.

For randomly oriented inclusions, the material behavior becomes isotropic. It is then assumed that there are equal numbers of fibers oriented in each direction, which is consistent from a probabilistic point of view, as no direction is favored. However, the stiffness value remains influenced by the aspect ratio. As before, cases with extreme aspect ratio values (i.e., $AR = 0.01$ and $AR = 10,000$) exhibit higher stiffness. As expected, we observe that for an aspect ratio equal to 1, the value obtained is identical in the randomly oriented and 11-oriented cases, since these are spheres, whose properties are independent of orientation. However, compared to the average stiffness of the unidirectional (UD) case, the randomly oriented case appears less efficient. In conclusion, the choice between these two configurations depends on the type of application. The unidirectional (UD) case favors stiffness in a specific direction while the randomly oriented case provides more consistent behavior in all directions.

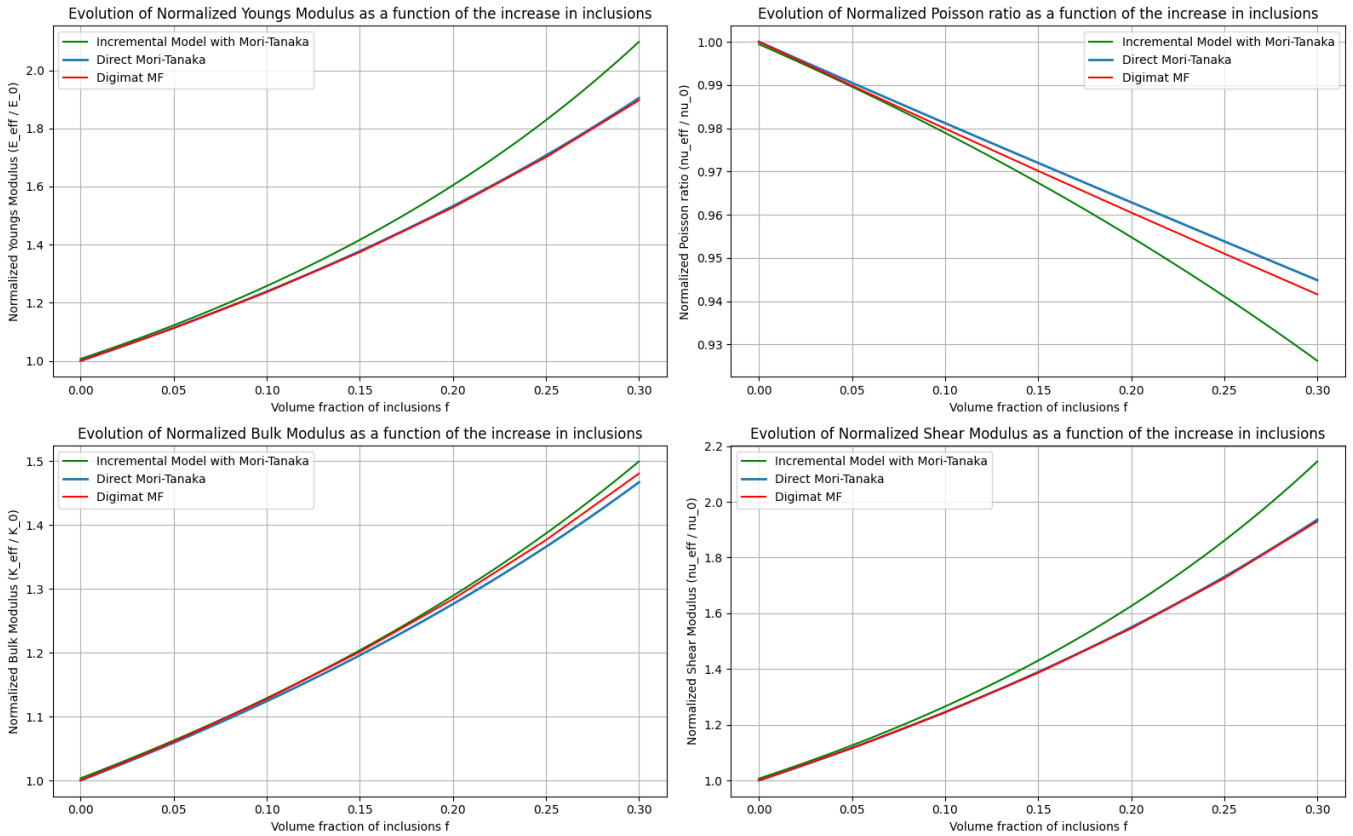

Figure 4: Comparison of the engineering constants between the three models

Above we can see the comparison between the results obtained via our and Digimat with an aspect ratio of 1, that is to say spherical inclusions. Although the incremental Mori-Tanaka method was selected in Digimat-MF, the results obtained were found to be very similar to those of the direct model used in part 1. After checking the parameters, this suggests that the implementation of the incremental method in Digimat-MF does not present any notable difference in the case of purely elastic behavior, even at a high inclusion rate (90%)... We will still note some differences for the Poisson ratio and the bulk Modulus. Finally, the values of the three models used for the different engineering constants are almost identical up to an inclusion rate of 10%.

Part 3: Full field homogenization for Polyamide lattice structure

In this section, we aim to determine the effective Young's modulus E from the stress-strain curves generated by Digimat. Surprisingly, the software does not directly provide the usual engineering constants. To circumvent this, we simulated different inclusion volume fractions (%) and extracted the slope of the stress-strain curves. The objective is to determine at which inclusion fraction the structure achieves equivalent or even improved isotropic stiffness. This analysis is crucial to understand how to optimize a lattice structure to benefit from both weight reduction and mechanical strengthening.

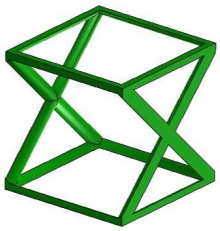

(a) Unit Cell Structure

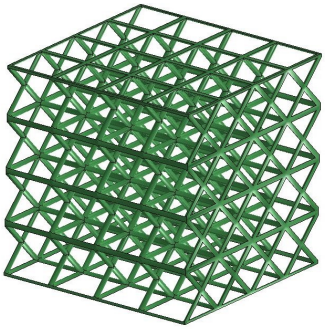

(b) Completed Lattice Structure

The figure on the left shows a unit cell of the truss structure, while the figure on the right illustrates the complete structure. Modeling a cube of $1.2m \times 1.2m \times 1.2m$ with beams of diameter $0.03m$ gives a volume of $0.11568m^3$, a 92% reduction in the total volume compared to a solid cube ($V = 1.44m^3$).

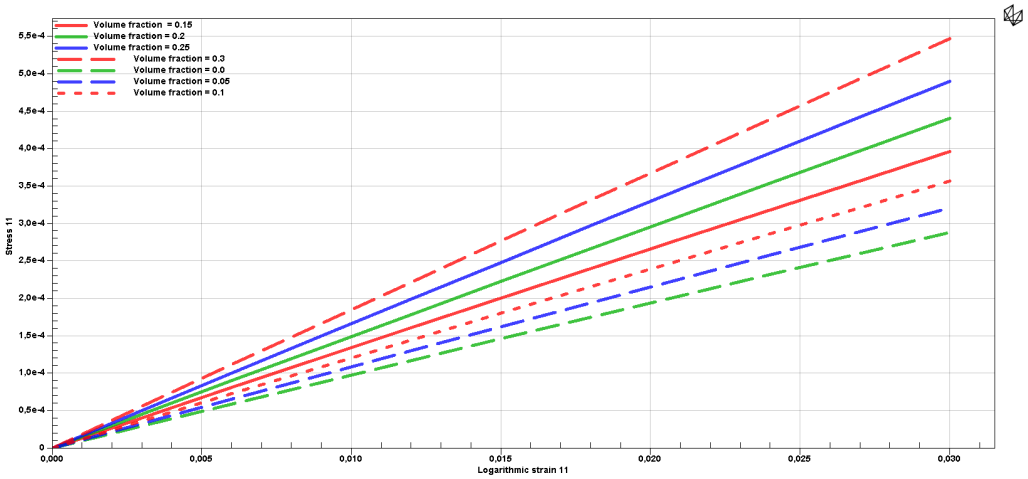

Figure 6: Strain vs Stress Graph

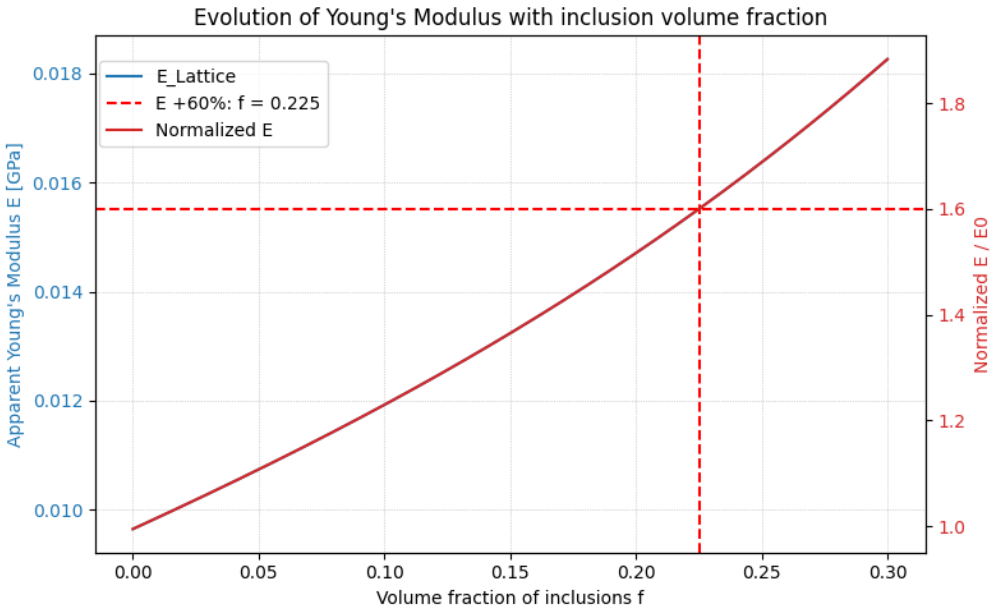

Figure 7: Evolution of Young's Modulus with inclusion volume fraction

Figure 6 presents the stress-strain curves obtained for different inclusion fractions. An increasing slope is observed with increasing inclusion percentage, reflecting an increase in stiffness. Figure 7 clearly shows that stiffness (effective Young's modulus) increases almost linearly with the inclusion volume fraction. At approximately 22.5% inclusion, a 60% increase in stiffness is achieved, which is consistent with the results from previous analyses.

% Inclusions	Strain	stress	Young's Modulus (GPa)
0.00	0.03	0.00029	0.0097
0.05	0.03	0.00032	0.0106
0.10	0.03	0.00036	0.0120
0.15	0.03	0.00039	0.0133
0.20	0.03	0.00044	0.0147
0.25	0.03	0.00049	0.0163
0.30	0.03	0.00055	0.0183

Table 3: Material properties with different models

The analysis demonstrates that the addition of inclusions significantly improves the rigidity of the structure, despite a significant reduction in density. This synergy between lightness and mechanical performance is particularly interesting for applications in lightweight engineering (aeronautics, biomechanics, etc...).

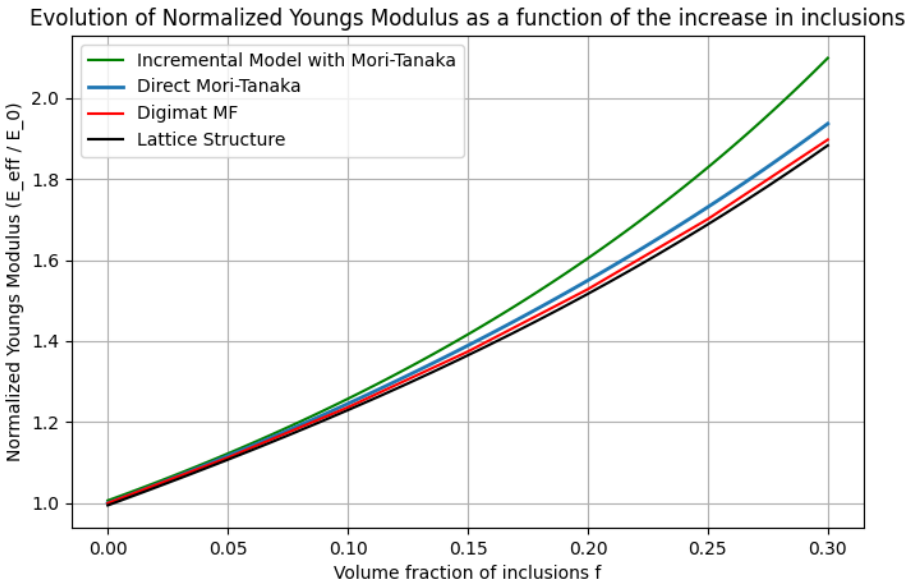

Figure 8: Comparison of the evolution of Young's Modulus

Ultimately, it is found that the normalized results obtained for the lattice structure correspond quite well to the direct Mori-Tanaka model. The slight difference between Digimat MF and the lattice structure comes from the fact that the stiffness values were calculated manually. It is also important to note that a 98% decrease in stiffness is observed for a 96% reduction in mass.

References

[1] Hubs, "What is FDM 3D printing?", 2023, Available: https://www.hubs.com/knowledge-base/what-is-fdm-3d-printing/. [Accessed: 28-Apr-2025]

[2] Aude Simar, Advanced Manufacturing course,2024, Available: Lecture notes, Université catholique de Louvain.

[3] Egan, P.F.; Khatri, N.R.; Parab, M.A.; Arefin, A.M.E., "Mechanics of 3D-Printed Polymer Lattices with Varied Design and Processing Strategies" *Polymers*, 2022. Available: https://www.mdpi.com/2073-4360/14/24/5515. [Accessed: 28-Apr-2025]

[4] 3D Systems, "SLA Stereolithography 3D Printing Service" *Dassault Systems*. Available: https://www.3ds.com/make/service/3d-printing-service/sla-stereolithography. [Accessed: 28-Apr-2025]

[5] Zian Jia, Fan Liu, Xihang Jiang, Lifeng Wang, "Engineering lattice metamaterials for extreme property, programmability, and multifunctionality." *J. Appl. Phys.*, 2020. Available: https://doi.org/10.1063/5.0004724. [Accessed: 28-Apr-2025]

[6] Duke University, "Metamaterials Explained Simply and Visually" *YouTube*, 2018, Available: https://www.youtube.com/watch?v=JH3YbgzUL-U. [Accessed: 28-Apr-2025]

[7] Sabine Hossenfelder, "Meta-Materials: Invisibility Cloaks, Superlenses, And Earthquake Protection" *YouTube*, 2023. Available: https://www.youtube.com/watch?v=iNugreoNuo0. [Accessed: 28-Apr-2025]

[8] Yehia, H.M.; Hamada, A.; Sebaey, T.A.; Abd-Elaziem, W. "Selective Laser Sintering of Polymers: Process Parameters, Machine Learning Approaches, and Future Directions." *J. Manuf. Mater. Process.* 2024, Available: https://doi.org/10.3390/jmmp8050197 [Accessed: 29-Apr-2025]